Synchronous reluctance motors with asymmetric rotor shapes and epoxy resin for electric vehicles

Andrea Credo
Dept. of Industrial and Information Eng. and Economics
University of L'Aquila
L'Aquila, Italy
andrea.credo@graduate.univaq.it

Marco Villani
Dept. of Industrial and Information Eng. and Economics
University of L'Aquila
L'Aquila, Italy
marco.villani@univaq.it

Mircea Popescu
Motor Design Limited
Wrexham, UK
mircea.popescu@motor-design.com

Nicolas Riviere
Motor Design Limited
Wrexham, UK
nicolas.riviere@motor-design.com

***Abstract*— This paper deals with the design of a Synchronous Reluctance motor for full-electric vehicle applications. In particular, the design is focused on premium vehicles and aims at the development of rare-earth free electric motor technologies featuring low cost manufacturing. Different solutions are proposed and compared with focus on the rotor design; the investigated topologies employ asymmetric rotor structures with "fluid shaped" barriers without radial ribs to maximize the average torque and minimize the torque ripple. As this choice is very critical for the mechanical strength of the rotor core at high speed, it has been decided to fill the flux barriers with epoxy adhesive resin. The use of the resin has required an accurate mechanical analysis in order to assess the rotor robustness at high speed.**

The paper presents the performances of the optimized design and the efficiency and torque ripple maps: moreover, useful information on the use of the epoxy resin in the synchronous reluctance motor are provided.

Keywords—Synchronous Reluctance Motor, Asymmetric shape, Radial ribs, Adhesive Epoxy Resin, Torque Ripple, Electric vehicle, Rare-earth free.

I. INTRODUCTION

The impact of internal combustion engine on the environment has led to many efforts to replace it with alternative propulsion systems, among which the electric machine has become the primary candidate [1]-[2]. In general, electric motors in powertrain applications need to meet several requirements and particularly: high torque and power density, high torque at low speed and high power at high speed, high efficiency, reliability, robustness and a reasonable cost.

The vast majority of motor solutions relies on high performance permanent magnets (PM), a technology based on rare-earth materials [3]-[4]. These machines have been subjected to extensive research for traction application due to their inherent advantages like high specific torque and low losses, which justify their adoption in most applications.

However, the manufacturers are focused on reducing the content of rare-earth magnets in electric machines used in electric vehicles. In fact, the high and volatile cost of raw materials for magnets makes uncertain their long-term availability, especially since the electric traction technology is called to be manufactured in mass production in the future transportation system.

Therefore, there is a growing attention in alternative solutions that include reduced rare-earth PM machines [5] or rare-earth free machines and several types of motors have been under study for propulsion applications.

The Synchronous Reluctance Motor (SynRM) is becoming of great interest in the recent years and represents a valid alternative for electric and hybrid vehicles for its simple and rugged construction.

The conventional SynRMs are known for their lower specific (peak) power and specific (peak) torque, higher noise and lower power factor. Despite these drawbacks, it is possible to improve the electromagnetic performance through an optimized design of the rotor geometry, reaching performances higher than the ones of an Induction Motor (IM) of the same size [6].

Moreover, high power and high-speed electric machines are the future trends in automotive applications and these traction machines have a significant mechanical stress. Therefore, it becomes essential to optimize the shape of flux barriers taking into account both mechanical and electromagnetic performance.

The aim of this paper is the design of a high speed SynRM for a full-electric premium vehicle and different solutions are proposed and compared with focus on the rotor design. The comparison has been carried out on the base of Finite Element (FE) analyses, considering the average torque, efficiency and torque ripple.

The investigated topologies employ asymmetric rotor structures with "fluid shaped" barriers without radial ribs to maximize the average torque and minimize the torque ripple. As this choice is very critical for the mechanical strength of the rotor core at high speed, it has been decided to fill the flux barriers with epoxy adhesive resin. This technological solution allows to improve the electro-mechanical performance of the machine and to minimize the cross-magnetization effects, thus improving the robustness of a possible sensorless control [7]-[8]. The use of the resin inside the barriers has required an accurate

mechanical analysis to verify if the rotor structure was able to withstand the mechanical stress at high speed. The results of this investigation are presented and discussed and useful information on the use of the resin in the synchronous reluctance motor are provided.

II. Design optimization

The design of the SynRM for traction requires accurate sizing procedures [9]-[12] that differ from the process of a traditional industrial machine, which is designed to mostly operate at a rated speed and torque. In traction motors, high performance and high efficiency are required over a wide speed range [13]; specific tools and optimization procedures should be used for the design refinements in order to satisfy the hard requirements without oversizing the machine [14].

The preliminary SynRM design with a symmetric rotor and fluid shape barriers has been sized using the Joukowsky equation as analytical expression for the shape of the barriers. The radius of the barrier curve is:

$$r(\theta) = r_{shaft} \sqrt[p]{\frac{c + \sqrt{c^2 + 4\sin^2(p\theta)}}{2\sin(p\theta)}} \qquad (1)$$

where:

r_{shaft} is the radius of the shaft

c is a constant and depends on the position of the barrier

p are the pole pairs

θ is the mechanical angle.

The shape of each barrier is characterized by two curves and each curve is defined by a proper constant *c*. Since the usage of the Joukowsky equation is a pre-optimization of the shape of the barriers, a preliminary design has been easily carried out. Then, different types of SynRMs with fluid shaped flux barriers have been optimized and compared and the main focus was on maximizing the average torque and minimizing the torque ripple. The latter is conventionally achieved by the rotor skewing in order to reduce the air-gap harmonics that produce a high torque ripple. In this paper, asymmetric rotor shapes have been adopted [15]-[16] without implementing the rotor skew technique.

The motor requirements are shown in TABLE I. and the specific torque, specific power and efficiency have been defined based on the Tesla Model-S full-electric car [17].

The designs have been carried out using an optimization algorithm [18] linked with a FE tool: it has been focused only on the rotor design and the following solutions have been investigated:

M1) symmetric rotor;

M2) asymmetric rotor 1;

M3) asymmetric rotor 2;

M4) double-asymmetric rotor.

The number of poles and the number of slots have been fixed to 6 and 54 respectively and also the stator core (Fig.1) and the distributed winding. The number of flux barriers has been chosen with respect to the n.poles/n.slots combination and 4 barriers per pole have been set. About the electrical steel, the commercial SiFe M235-35A material (thickness of 0.35 mm) has been selected.

TABLE I. Motor Requirements for the Target Application

Requirements	***Unit***	***Value***
DC Voltage	V	800
Specific Peak Power	kW/kg	> 4.0
Specific Peak Torque	Nm/kg	> 8.0
Peak Power @ 5000 rpm	kW	> 200
Peak Torque @ 5000 rpm	Nm	> 380
Peak Efficiency	%	> 95
Maximum Speed	rpm	16000
Power @ Maximum Speed	kW	> 70
Torque Ripple	%	< 15
Outer Stator Diameter	mm	230
Stack Length	mm	200
Air-gap Length	mm	0.70
Motor Mass (active materials)	kg	< 48

The optimization was aimed to maximize the torque and to minimize the torque ripple at high speed (16000 rpm): the constraints concerned the minimum value of peak torque (at 5000 rpm) and the maximum values of the voltage at peak power and maximum speed.

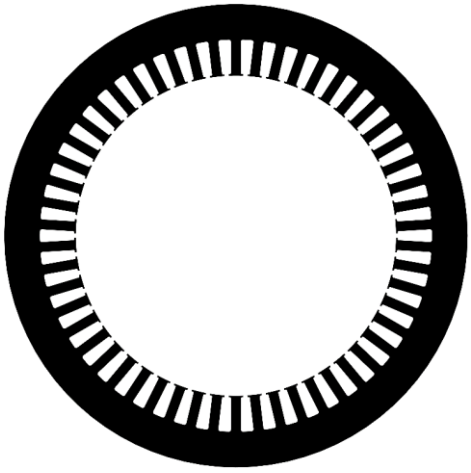

Fig. 1. Cross section of the stator core.

Fig. 2 shows the optimized rotor of the M1 design: the flux barriers of the two adjacent poles have the same dimensions and the same shape. Fig. 3 presents the torque behaviors, by FE analyses, both for the peak power and the maximum speed (16000 rpm) operations.

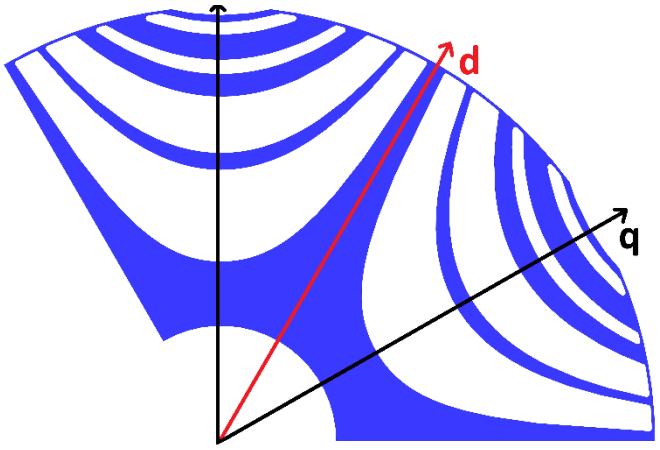

Fig. 2. M1 design: cross section of the symmetric rotor (2 poles).

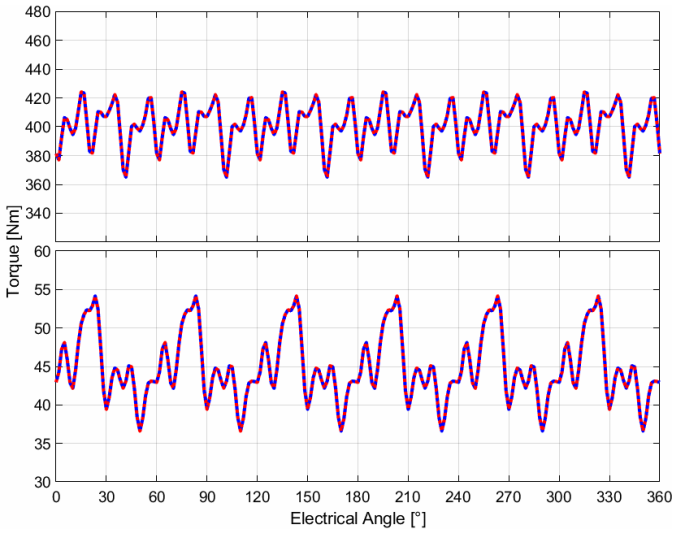

Fig. 3. M1 design: Torque vs. rotor position at peak Power (upper) and max Speed (lower) operations.

The rotor of the optimized design M2 (Fig.4) is similar to the one of the M1 design but it has an asymmetric pole structure to compensate the torque harmonics: particularly, the rotor shape is asymmetric on the q-axes but it is the same for each pole.

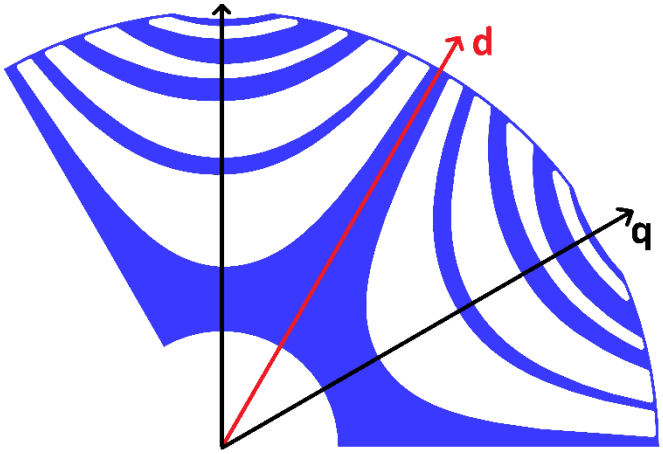

Fig. 4. M2 design: cross section of the asymmetric rotor (2 poles).

The torques have been calculated considering the clockwise rotation (traction mode) and counter-clockwise rotation (reverse gear), and this is due to the particular asymmetry of the rotor structure: Fig. 5 points out a different trend on the torque profiles both for the peak power operation and the maximum speed operation.

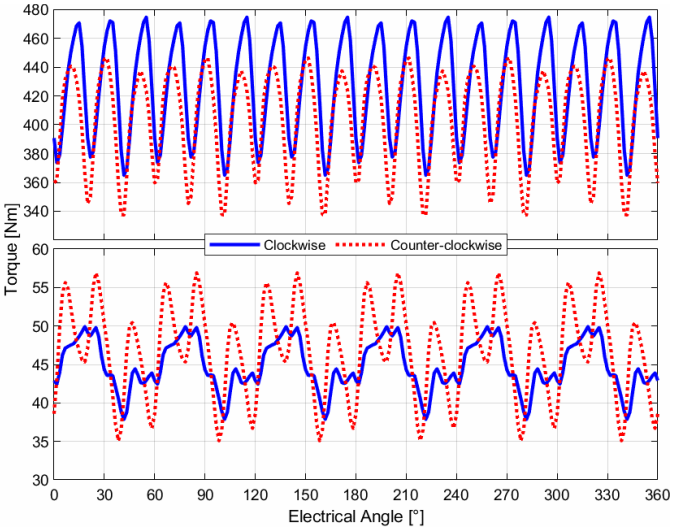

Fig. 5. M2 design: Torque vs. rotor position at peak Power (upper) and max Speed (lower) operations.

The rotor shape of the M3 design is shown in Fig. 6: it has two adjacent different poles due to the position of the flux barriers. The torque profiles are presented in Fig. 7 and the curves with clockwise and counter-clockwise rotations are perfectly coincident.

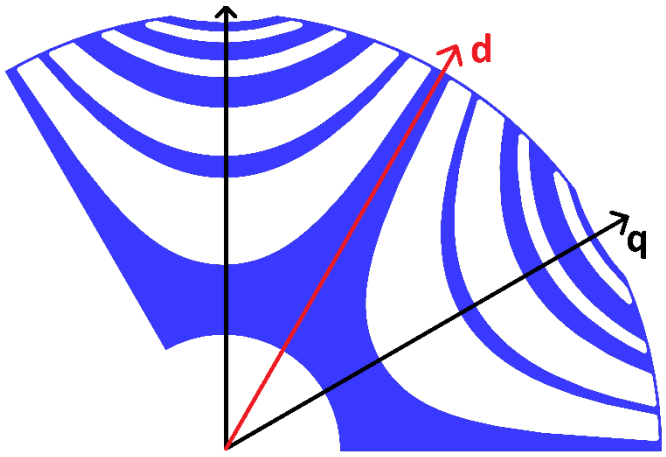

Fig. 6. M3 design: cross section of the asymmetric rotor (2 poles).

The optimized rotor of the M4 design (Fig. 8) can be seen as a combination between M2 and M3 solutions and it presents two different asymmetric consecutive poles with a double asymmetry either about the q-axes and respect two adjacent poles. It is also evident a different profile of the external barrier close to the air-gap. The torque behaviours for the clockwise and counter-clockwise rotations are shown in Fig. 9.

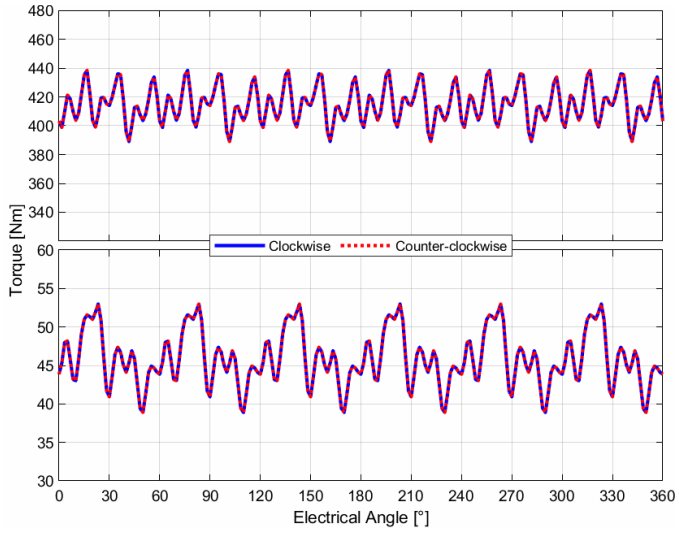

Fig. 7. M3 design: Torque vs. rotor position at peak Power (upper) and max Speed (lower) operations.

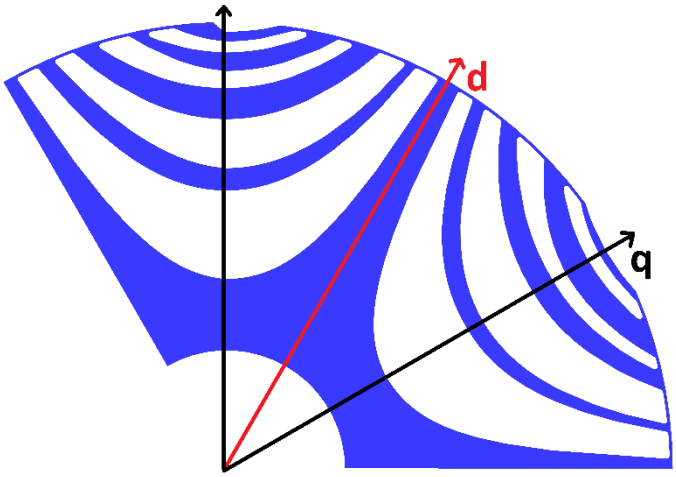

Fig. 8. M4 design: cross section of the asymmetric rotor (2 poles).

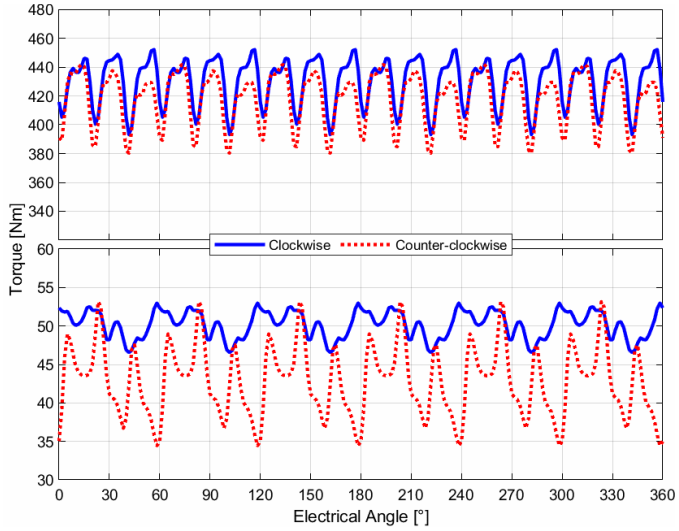

Fig. 9. M4 design: Torque vs. rotor position at peak Power (upper) and max Speed (lower) operations.

The performances of the proposed designs are compared in TABLE II: in bold the values that do not meet the requirements. The designs fully satisfy the specific peak torque, peak power and power at maximum speed. M1 and M2 are not able to satisfy the torque ripple requirements while M3 guarantees a good ripple only at the base speed. The design M4 presents the best performance in terms of power at base and maximum speeds with a reasonable torque ripple.

TABLE II. OPTIMIZED DESIGNS

Performance	***Unit***	***M1***	***M2***	***M3***	***M4***
Specific Peak Power	kW/kg	4.3	4.6	4.4	4.6
Specific Peak Torque	Nm/kg	8.6	9.1	8.9	9.2
Peak Power @ 5000 rpm	kW	201	214	208	216
Torque Ripple @ 5000 rpm	%	**15.4**	**21.2**	8.8	9.7
Power @ Max Speed (16000 rpm)	kW	75	75	76	84
Torque ripple @ Max Speed (16000 rpm)	%	**39**	**27**	**31**	12
Motor Mass (active materials)	kg	47	47	47	47

The particular asymmetric shape of the barriers for the designs M2 and M4 affects the rotation direction of the rotor: it means that the motor must operate with the clockwise rotation (traction mode) in order to exploit the advantage of the rotor shapes on the maximum torque available and the minimum torque ripple. This requirement is not critical in automotive applications, where good performances are required during the traction and not in reverse gear or braking operations.

In Fig. 5 and Fig. 9 it is clear how the rotation direction significantly affects the mean torque value and the torque ripple for the designs M2 and M4. The design M3 shows the same trends of the torque curves both with clockwise and counter-clockwise rotations (Fig. 7).

The M4 design fully satisfies the requirements and appears to be a good solution with a smooth torque behavior for the clockwise rotation: the torque ripple is 12% at maximum speed and about 10% at peak power and base speed. This design has been further analyzed in order to verify the mechanical strength of the rotor core at high speed.

III. MECHANICAL ANALISYS

The design M4 is very promising for automotive applications but the rotor without radial ribs does not assure high-speed operations. In order to improve the mechanical strength, the flux barriers have been filled with adhesive epoxy resin. The chosen commercia resin is the liquid aluminum-filled WEICON® C and the main characteristics are listed in TABLE III: it is a liquid resin, anti-magnetic, without shrinkage and it has a good temperature resistance (up to +220°C). This resin is particularly suitable as an adhesive for large-scale applications with a high thermal stress.

TABLE III. EPOXY RESIN PROPERTIES

Characteristic	*Unit*	*Value*
Density	kg/m^3	1620
Young Module	GPa	5.8 – 6
Compressive Strength	Mpa	140
Tensile Strength	Mpa	25
Bending Strength	Mpa	77
Shrinkage	%	0.01
Maximum Layer Thickness	mm	60
Temperature Resistance	°C	220
Maximum Adhesive Strength	Mpa	12

This technological solution (rotor with resin) has required an accurate FE mechanical analysis to verify if the rotor structure was able to withstand mechanical stresses at high speed. For this type of analysis, a fine mesh has been adopted (Fig. 10) to simulate accurately the stresses inside the rotor. The analysis has been focused on the maximum speed (16000 rpm) in order to test the contact between the resin and the electrical steel.

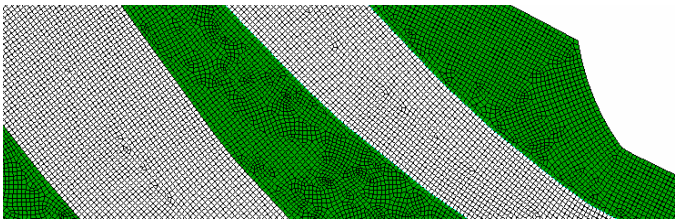

Fig. 10. Detail of the mesh for the mechanical analysis.

Fig. 11 presents the equivalent stresses inside the electrical steel only. The maximum stress, located in the tangential ribs, is lower than 480MPa (that is the limit for the chosen M235-35A steel), but this value could be affected by the variation of the mechanical properties along with the temperature and possible inaccuracy due to the manufacturing process (shearing, punching). The stress can be reduced by increasing the thickness of the radial ribs (but this affects the motor performance) or adopting an epoxy resin with a higher Young module (if available on the market).

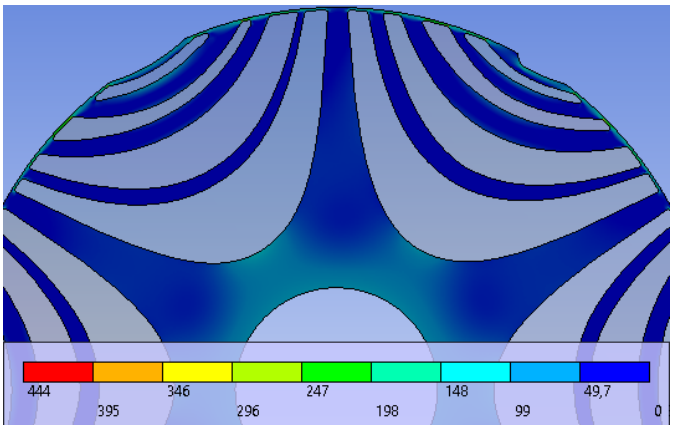

Fig. 11. M4 design: equivalent stresses inside the electrical steel @ 16000 rpm (in MPa).

Fig. 12 shows the equivalent stresses inside the resin. It is clear that the epoxy resin works under the 50% of its mechanical limit (25 MPa) guaranteeing a good safety for the structural integrity. The maximum stresses are located on the barriers close to the shaft because they have to support also the mass of the other barriers.

Fig. 13 and Fig. 14 show the contact pressure and frictional stresses between resin and electrical steel.

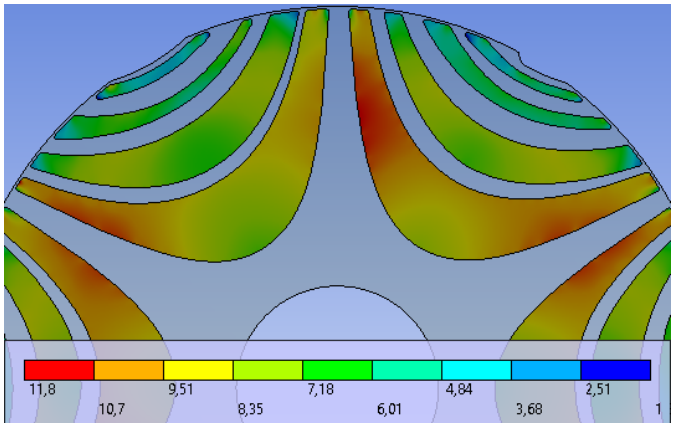

Fig. 12. M4 design: equivalent stresses inside the resin @ 16000 rpm (in MPa).

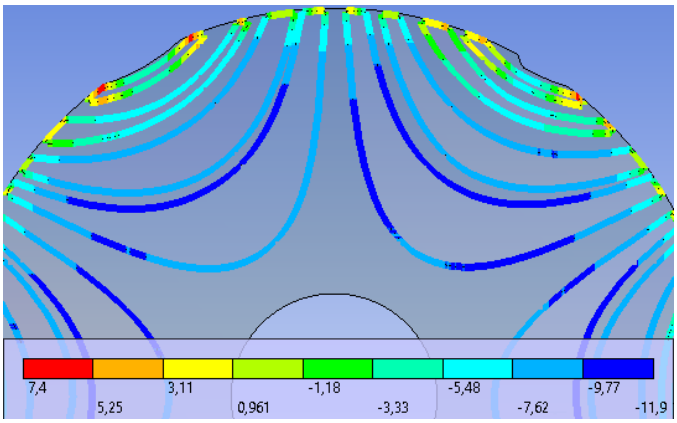

Fig. 13. M4 design: contact pressure between the resin and the electrical steel @ 16000 rpm (in MPa).

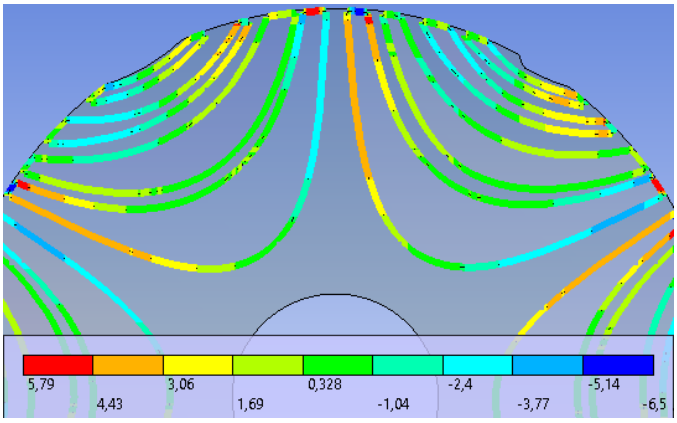

Fig. 14. M4 design: frictional stresses between the resin and the electrical steel @ 16000 rpm (in MPa).

The negative value of the contact pressure means that the steel and the resin are moving off and the contact could be not guaranteed. The values of the frictional stresses are reasonable for this application. For the contact pressure the results are critical and close to the limit of the epoxy resin (the max adhesive strength is 12 MPa); this could cause the resin to detach from the barrier with consequent weakening of the rotor structure at high speed. The use of a resin with higher adhesive strength could overcome this criticality.

Fig. 15 shows the deformation of the external part of the rotor close to the air-gap at 16000 rpm: the peak value is reasonable and about 13% of the airgap length (0.70 mm) and ensures the correct motor operation.

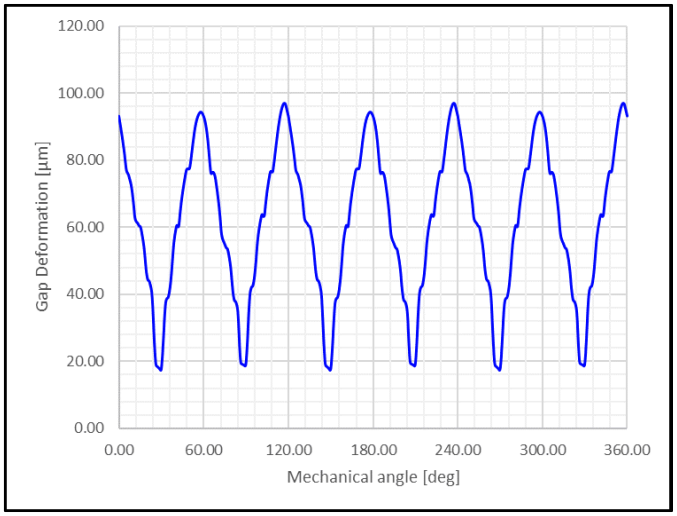

Fig. 15. M4 design: air-gap deformation vs. mechanical angle @ 16000 rpm.

The mechanical analysis has allowed to test the robustness of the rotor core without radial ribs and to verify the limit of the chosen commercial resin at high speed. The results point out that the rotor structure with the resin is able to withstand mechanical stresses even if some critical points are highlighted inside the flux barriers at 16000 rpm. The use of a more performing epoxy resin (if available on the market) could guarantee a good mechanical strength at very high speed.

IV. Efficiency and Torque Ripple Maps

The efficiency maps of the optimized M4 design are shown in Fig. 16 for either positive and negative torque values. These maps have been calculated by FE analyses by setting a "maximum efficiency" control strategy.

The maps are slightly different and this is due to the asymmetric rotor structure that has been optimized, favoring the clockwise rotation (for the traction mode and not in the reverse gear): the peak efficiency is 96%. Fig. 16 points out that the maximum positive torque is higher than the negative one even during the flux-weakening operation.

The maps reported in Fig. 17 show the torque ripple in the torque-speed plane with the same control strategy adopted for the calculation of the efficiency maps.

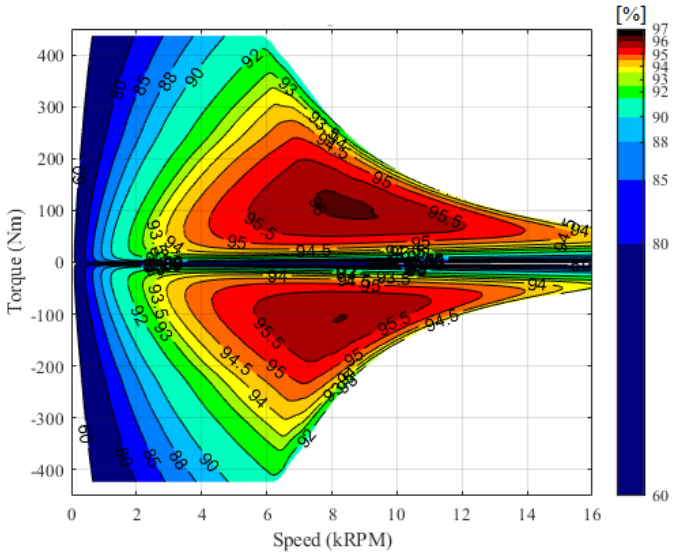

Fig. 16. M4 design: efficiency maps.

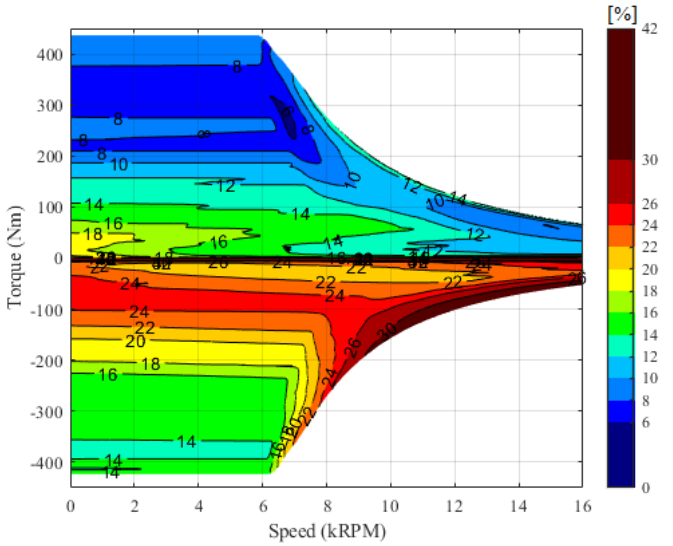

Fig. 17. M4 design: torque ripple maps.

The use of an asymmetric rotor shape has allowed a significant ripple reduction in the clockwise direction with positive torque (traction mode), but not in the opposite one in accordance with what has been imposed during the optimization steps: this reduction is due mainly to the accurate rotor design without skewing. Moreover, the area with low ripple values (about 6%) is close both to the peak torque and the maximum speed, while the region with negative torque (reverse gear) presents higher torque ripple (about 40%), particularly at maximum speed: this value is not critical considering the short duration of this operation.

V. Conclusions

High power and high-speed electric machines are the future trends in automotive applications and these traction machines have significant mechanical stress. Therefore, it becomes essential to optimize the motor design taking into account both mechanical and electromagnetic performances.

In this paper the design of a Synchronous Reluctance motor for a full-electric vehicle has been presented and different topologies with symmetric and asymmetric rotor shapes have been designed, optimized, and compared. The investigated solutions employ rotor structures with “fluid shaped” barriers without radial ribs to maximize the torque and to minimize the torque ripple. As this choice is very critical for the mechanical strength of the rotor core at high speed, it has been decided to fill the flux barriers with epoxy adhesive resin. In this study, a commercial resin has been chosen and an accurate mechanical analysis has been carried out to verify the rotor robustness at high speed.

The performances of the proposed solution are satisfactory in terms of efficiency and power density, but the mechanical analysis has highlighted some critical issues at high speed. The use of high performance epoxy resin (if available on the market) could certainly make it possible to overcome the mechanical constraints.

In conclusion, the SynRM can be considered a valid alternative to other rare-earth free or reduced earth-free solutions and can compete on the market for the development of new generations of electric vehicles.

ACKNOWLEDGMENT

This project (ReFreeDrive) has received fundings from the European Union's Horizon 2020 research and innovation programme under the Grant Agreement No (770143)

REFERENCES

[1] C.C.Chan, “The State of the Art of Electric and Hybrid Vehicles”, Proceeding of IEEE, vol. 90, no. 2, February 2002, pp. 247-275.

[2] Z. Q. Zhu, D. Howe, “Electrical Machines and Drives for Electric, Hybrid, and Fuel Cell Vehicles”, Proceedings of the IEEE, vol. 95, no. 4, April 2007, pp. 746-765.

[3] K. T. Chau, C. C. Chan, Chunhua Liu, “Overview of Permanent-Magnet Brushless Drives for Electric and Hybrid Electric Vehicles”, *IEEE Transaction on Industrial Electronics*, vol. 55, no.. 6, June 2008, pp. 2246-2257.

[4] M.Burwell, J.Goss, M.Popescu, “Performance/cost comparison of induction motor & permanent magnet motor in a hybrid electric car”, International Copper Association, July 2013, Tokyo.

[5] J. D.Widmer , R. Martin, M. Kimiabeigi, “Electric vehicle traction motors without rare earth magnets”, Sustainable Materials and Technologies, Elsevier, 3 (2015), pp. 7-13.

[6] M. Villani, M. Tursini, M. Popescu, G. Fabri, A. Credo, L. Di Leonardo “Experimental Comparison between Induction and Synchronous Reluctance Motor-Drives” ICEM 2018, XXIII International Conference on Electrical Machines, Alexandroupoli (Greece), September 2018,

[7] W. Villet and M. Kamper, "Variable-gear EV reluctance synchronous motor drives—An evaluation of rotor structures for position-sensorless control," *IEEE Trans. Ind. Electron.*, vol. 61, no. 10, pp. 5732-5740, 2014.

[8] M. Tursini, M. Villani, G. Fabri, S. Paolini, A. Credo and A. Fioravanti, "Sensorless control of a synchronous reluctance motor by finite elements model results", SLED IEEE International Symposium on Sensorless Control for Electrical Drive, Catania (Italy), September 2017.

[9] M. Ferrari, N. Bianchi, A. Doria and E. Fornasiero, "Design of Synchronous Reluctance Motor for Hybrid Electric Vehicles", *IEEE Transactions on Industry Applications*, vol. 51, no. 4, pp. 3030-3040, 2015.

[10] G. Pellegrino, F. Cupertino and C. Gerada, "Automatic Design of Synchronous Reluctance Motors Focusing on Barrier Shape Optimization", *IEEE Transactions on Industry Applications*, vol. 51, no. 2, pp. 1465-1474, 2015

[11] F.Parasiliti, M.Villani “Magnetic analysis of flux barriers Synchronous Reluctance Motors” ICEM 2008, XVIII International Conference on Electrical Machines, Vilamoura (Portugal), September 2008.

[12] S. Taghavi, P. Pillay, “A Sizing Methodology of the Synchronous Reluctance Motor for Traction Applications“, IEEE Journal of Emerging and Selected Topics in Power Electronics, Vol.. 2, No. 2, June 2014.

[13] I. Boldea, L. Tutelea, L. Parsa and D. Dorrell, "Automotive Electric Propulsion Systems With Reduced or No Permanent Magnets: An Overview", *IEEE Transactions on Industrial Electronics*, vol. 61, no. 10, pp. 5696-5711, 2014.

[14] M. Tursini, M. Villani, G. Fabri, A. Credo, F. Parasiliti and A. Abdelli, "Synchronous Reluctance Motor: Design, Optimization and Validation", 2018 International Symposium on Power Electronics, Electrical Drives, Automation and Motion (SPEEDAM), 2018.

[15] N.Bianchi, S.Bolognani, D.Bon, M Dai Pre, “Rotor Flux-Barrier Design for Torque Ripple Reduction in Synchronous Reluctance motor”, in Conf. Record of the 2006 IEEE 41st, Ind. Appl. Annual Meeting, Tampa, vol.3, pp.1193-1200.

[16] E.Howard, M.J.Kamper, S.Gerber, “Asymmetric Flux Barrier and Skew Design Optimization of Reluctance Synchronous Machines”, *IEEE Transactions on Industry Applications*, vol. 51, no. 5, pp. 3751-3760, 2015.

[17] Tesla Model S Pricing and Specs Revealed, MotorWard, 2011 [Online]. Available : http ://www.motorward.com/2011/12/teslamodel-s-pricing-and-specs-revealed/

[18] S.Lucidi, F.Parasiliti, F.Rinaldi, M.Villani “Finite Element Based Multi-Objective Design Optimization Procedure of Interior Permanent Magnet Synchronous Motors for Wide Constant-Power Region Operation”, IEEE Trans. on Industrial Electronics, vol. 59, p. 2503-2514, ISSN: 0278-0046.